Si and Be intralayers at GaAs/AlAs heterojunctions: Doping effects

M. Moreno,* J. L. Sacedón, and M. Alonso
Instituto de Ciencia de Materiales de Madrid (CSIC), Cantoblanco, E-28049 Madrid, Spain

M. Höricke and R. Hey
Paul-Drude-Institut für Festkörpelektronik, Hausvogteiplatz 5-7, D-10117 Berlin, Germany

J. Avila and M. C. Asensio
LURE, Centre Universitaire Paris-Sud (Bâtiment 209D), F-91405 Orsay Cédéx, France

K. Horn
Fritz-Haber-Institut der Max-Planck-Gesellshaft, Faradayweg 4-6, D-14195 Berlin, Germany

K. H. Ploog
Paul-Drude-Institut für Festkörpelektronik, Hausvogteiplatz 5-7, D-10117 Berlin, Germany
(Received 16 April 1998)

Experimental studies that suggest the possibility to ''engineer'' band offsets in semiconductor heterojunctions by means of intralayers have been controversially discussed. Here, Si and Be insertions at GaAs-on-AlAs(100) interfaces are investigated by photoelectron spectroscopy (PES) using synchrotron radiation. Our aim is to clarify the effect that band bending imposes on the determination of interface band offsets. The Ga($3d$)-to-Al($2p$) core-level energy separation is found to increase upon Si insertion, and to decrease upon Be insertion. The surface Fermi level moves closer to the valence-band maximum in Si-containing samples, while it moves away in Be-containing ones. These results are consistent with the *n*-type and *p*-type doping behaviors typically exhibited by Si and Be impurities in GaAs(100). The observed core-level offset variations support an interpretation based on band-bending arguments, rather than on the commonly invoked band-offset changes. A simple ''overlayer-capacitor'' model is proposed to illustrate the physical origin of such band-bending effects. [S0163-1829(98)08643-3]

I. INTRODUCTION

The insertion of Si layers into III-V semiconductors is motivated by two technological interests: (i) control of band offsets at heterointerfaces,[1] and (ii) generation of a two-dimensionally-confined electron gas within a δ-doped layer.[2–4] For both applications the insertion is performed using similar molecular-beam-epitaxy (MBE) procedures. However, the inserted impurities may play different roles depending on the concentration and atomic configuration of the intralayer. The ideal (100) surface of GaAs contains 6.26×10^{14} atoms cm^{-2}. The δ-doping concept deals with Si concentrations typically below/around 10^{13} atoms cm^{-2}, so that Si atoms have a doping role, some electrons being released to the host semiconductor lattice. Band-offset control was first attempted through *doping-related* methods, like the doping interface dipole (DID),[5] quantum interface-induced dipole (QUID),[6] and modulation-doping plus compositional-grading[7] methods. Later, *intralayer-induced interface-dipole* methods were proposed, where intralayer concentrations reaching the monolayer level (10^{14} atoms cm^{-2}) are required.[8,9] Although in this case most Si electrons remain localized close to Si cores, the intralayer insertion induces some charge displacement around the interface, resulting in the formation of microscopic interface dipoles.[10]

Photoelectron spectroscopy (PES) is widely used to determine valence-band offsets at heterointerfaces.[11] This technique measures the kinetic energy of electrons originally located inside the solid that have escaped from it due to light excitation. Such kinetic energy is directly related with the binding energy of the electrons in the solid. The valence-band discontinuity at semiconductor heterointerfaces (ΔE_V) can be derived from the energy offset measured between two core levels from each side of the interface (ΔE_{CL}). The strong scattering suffered by electrons moving inside matter causes the PES signal to rapidly attenuate with depth. Therefore, in order to determine band offsets, it is necessary for the interface to be located close enough to the surface, so as to permit the detection of the signal coming from the buried layer of the heterostructure. However, the band-offset determination by core-level PES is accurate only if energy levels do not suffer energy variations along the photoemission probing depth. If chemical reactions take place, or if bands are bent close to the surface, the data analysis should be carried out with great care, since these effects may broaden and/or shift the core-level peaks, which may lead to inaccuracies. Therefore, the valence-band offset directly determined from the core-level offset measured by PES is sometimes called the *apparent* offset (ΔE_V^*); it equals the *real* offset (ΔE_V) only if the energy values derived from PES data actually correspond to the energy values at the *interface*.

Using PES, Sorba *et al.* have studied the effect of Si intralayers at GaAs-AlAs polar heterojunctions,[12] and Marsi *et*

al. at GaAs-GaAs polar homojunctions.[13] Their experimental results were interpreted as a demonstration of the band-offset tuning effect predicted by theory.[8,9] However, criticisms of this interpretation have argued that such PES results could actually be connected with the existence of a sharp overlayer band bending.[14,15] In fact, the interpretation in terms of band-offset changes within the framework of the ''microscopic interface-capacitor'' model[10] does not provide a consistent explanation for all of the experimental results already reported. For instance, the absolute value of the intralayer-induced ΔE_V change was predicted, according to this model, to monotonically increase with intralayer thickness, at least up to intralayers 2 ML thick;[9] however, the effect has been experimentally observed to saturate at submonolayer concentrations, the largest change being obtained for intralayers about 1/2 ML thick.[12] Moreover, the microscopic interface-capacitor model emphasizes that band-offset changes can be achieved only if the interface has a *polar* geometry;[10,16] however, core-level offset variations have been observed on polar and nonpolar interfaces.[15,17] Thus, intralayer-induced band-offset modifications have not yet been rigorously demonstrated on these systems, because of the lack of a direct and truly local technique able to measure band offsets.

By relying solely on PES, it is difficult to assess whether the variations observed in the Al($2p$)-to-Ga($3d$) energy separation upon Si insertion at GaAs/AlAs junctions are due to a modification of the interface *band offset*, or to a variation of the *band-bending profile* near the surface. Such band-bending effects are not easily measurable, or even detectable, by photoemission spectroscopy.[18,19] However, investigating the insertion of intralayers with different doping behaviors may help to elucidate which is the correct interpretation of the core-level PES results. This paper reports on the effect of inserting Si and Be intralayers into GaAs-on-AlAs(100) heterojunctions, as investigated by PES using synchrotron radiation. Silicon exhibits an amphoteric doping behavior in GaAs that depends on growth conditions; under the standard GaAs(100) growth conditions Si behaves as a donor impurity. Beryllium is the impurity most commonly employed to obtain *p*-type doping in GaAs. If core-level offsets were actually modified by variations of the band profile, then one should expect changes of opposite sign for Si and Be intralayers, since *n*-type and *p*-type impurities induce band bendings of opposite sign. On the other side, according to Harrison's ''microscopic interface-capacitor'' picture,[10] band-offset changes are expected to occur in polar III-V/III-V heterointerfaces [such as GaAs-AlAs(100)] upon insertion of a group-IV intralayer (like Si), but it is not *a priori* clear which should be the effect for insertion of a group-II intralayer (like Be). Note that, within Harrison's model, the amphoteric behavior of the intralayer plays a key role in explaining the band-offset changes: the group-IV intralayer becomes positively ionized at the anion-terminated side of the interface (III-V/IV), whereas it becomes negatively ionized at the cation-initiated side (IV/III-V). Within this context, a III-V/III-V isovalent polar interface with a group-IV intralayer can be viewed as a pair of III-V/IV heterovalent interfaces, acting as the parallel plates of a microscopic capacitor. In particular, the microscopic interface-capacitor model predicts an increase of the band-offset at GaAs-on-AlAs(100) interfaces upon Si insertion. For the case of Be intralayers, detailed calculations of the charge transfer at the interface would be required for any prediction on band-offset changes. By comparing the effects of inserting Si and Be intralayers, the present study aims at clarifying the effect that band bending imposes on the determination of interface band offsets. Within this context, the possible modifications of the Fermi-level surface pinning-position induced by the Si and Be insertions are also examined.

II. EXPERIMENT

The GaAs/AlAs heterojunctions of the present study were grown by molecular-beam epitaxy (MBE); the growth parameters employed are summarized in Table I. We used epi-ready heavily Si-doped GaAs substrates ($n=1\times10^{18}$ cm^{-3}), with a (100)-2° off toward (111)A orientation. First, a 0.3-μm-thick Si-doped GaAs buffer layer was grown ($n=1\times10^{18}$ cm^{-3}), followed by a 20-nm-thick undoped AlAs layer. At this point, a layer of Si or Be with a density of 2.2×10^{14} atoms cm^{-2} [about 1/3 of the atomic sites in a (100) monolayer] was inserted in some samples. Finally, all samples were terminated by a 2-nm-thick, nominally undoped, GaAs layer. Growth rates were calibrated using RHEED (reflection high-energy electron diffraction) specular-beam intensity oscillations. Si and Be fluxes were determined by CV (capacitance-voltage) profiling measurements performed on homogeneously doped GaAs calibration layers. The substrate temperature during growth was measured using a thermocouple, placed at the back of the substrate holder, which was calibrated by taking as a reference point the temperature of the GaAs oxide desorption [580 °C on GaAs(100)]. Si and Be insertions were performed following a δ-doping protocol different from the conventional method used in previous PES studies. The method we have used combines a pulsed low-flux impurity-deposition technique, and the employ of a slight substrate misorientation [2° off toward (111)A]. This has been shown to improve the structural quality and the doping efficiency for insertion of Si layers in GaAs(100).[20,21] Growth of GaAs overlayers in samples containing a Si or a Be intralayer was performed at a reduced substrate temperature to minimize segregation and out-diffusion of intralayer atoms.

The samples were analyzed by PES, using synchrotron radiation coming from the TGM6 and TGM2 beam lines of BESSY I (*Berliner Elektronenspeicherring-Gesellschaft für Synchrotronstrahlung mbH*), and from the SU6 beam line of LURE (*Laboratoire pour l'Utilisation du Rayonnement Electromagnétique*). Electron kinetic-energy distribution curves (EDC) were recorded for each sample. We used a heavily doped substrate to prevent the samples from being charged during the photoemission analysis. The Ga($3d$), Al($2p$), As($3d$), and valence-band-edge emissions from the heterojunctions, as well as the Fermi-edge emission from a gold foil (in electrical contact with the semiconductor samples) were recorded at a fixed photon energy. This procedure was repeated for several photon energies. Electrons were collected and counted in the normal-emission geometry by an angle-resolving analyzer. The overall energy resolution was 150–300 meV in the range of photon energies used (40–95 eV).

Samples analyzed at BESSY I were vacuum-transferred

TABLE I. MBE-growth parameters of the different types of samples analyzed here.

	GaAs/AlAs(100)	GaAs/Si/AlAs(100)	GaAs/Be/AlAs(100)
Substrate			
orientation	(100)-2°→(111)*A*	(100)-2°→(111)*A*	(100)-2°→(111)*A*
Si doping	1×10^{18} cm^{-3}	1×10^{18} cm^{-3}	1×10^{18} cm^{-3}
Buffer layer			
thickness	0.3 μm	0.3 μm	0.3 μm
T (substrate)	590 °C	590 °C	590 °C
growth rate	0.2 μm/h	0.2 μm/h	0.2 μm/h
Si doping	1×10^{18} cm^{-3}	1×10^{18} cm^{-3}	1×10^{18} cm^{-3}
Buried layer (AlAs)			
thickness	20 nm	20 nm	20 nm
T (substrate)	610 °C	610 °C	610 °C
growth rate	0.2 μm/h	0.2 μm/h	0.2 μm/h
Si doping			
Intralayer			
2D density		2.2×10^{14} Si atoms cm^{-2}	2.2×10^{14} Be atoms cm^{-2}
T (substrate)		590 °C	500 °C
flux(pulsed)		2×10^{11} cm^{-2} s^{-1}	2×10^{11} cm^{-2} s^{-1}
Overlayer (GaAs)			
thickness	2 nm	2 nm	2 nm
T (substrate)	610 °C	540 °C	450 °C
growth rate	0.2 μm/h	0.2 μm/h	0.2 μm/h
Si doping			

from the MBE growth-chamber to the photoemission analysis chamber, at the synchrotron installation, by using a small UHV chamber with a base pressure in the high-10^{-10}-mbar range. All PES measurements were performed during the first week following the MBE sample growth. The samples and a gold foil were placed together in the analysis chamber, under electrical contact and grounded. We used a multiple sample holder that accommodated several samples, so that they could be measured consecutively under the same experimental conditions.

III. RESULTS

The band offset at GaAs-AlAs heterojunctions can be determined by measuring the energy separation between their Ga($3d$) and Al($2p$) core-level emissions. Spectra of this type recorded in BESSY I are shown in Fig. 1 for GaAs-on-AlAs(100) heterostructures with and without a Si intralayer (open and solid symbols, respectively). The Al($2p$) and Ga($3d$) core-level spectra have been area normalized, that is, the peaks compared have the same area. The spectra are displayed without performing any kind of energy alignment, so as the Fermi energy coincides for both samples. The core-level spectra from both types of heterostructures, and the Fermi-edge reference spectrum from the gold foil were recorded consecutively under the same experimental conditions, so that the results can be directly compared. We used 95-eV photons; at this photon energy, the Ga($3d$) emission is recorded with a high surface sensitivity, while the Al($2p$)

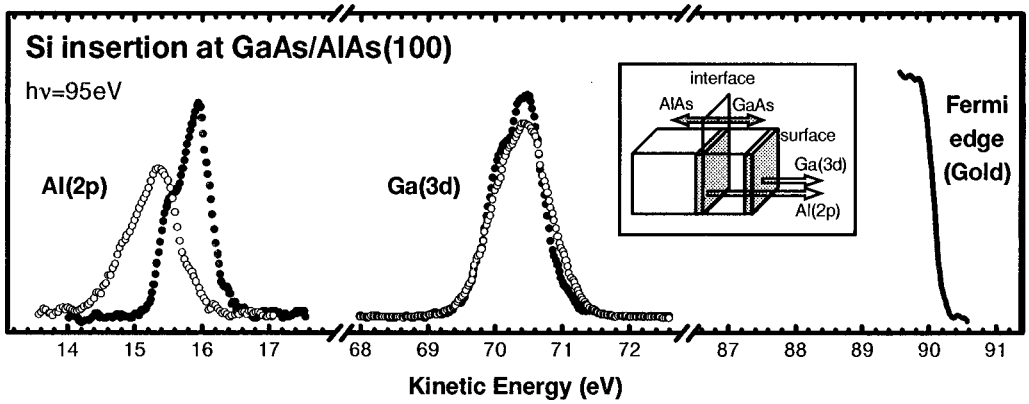

FIG. 1. Al($2p$) and Ga($3d$) EDC spectra recorded with 95-eV photons on GaAs/AlAs(100) (solid circles) and GaAs/Si/AlAs(100) (open circles) heterojunctions (GaAs on top). The gold Fermi-edge spectrum is also displayed for reference. The nominal concentration of the Si intralayer is 2.2×10^{14} atoms cm^{-2}, which corresponds to 1/3 of a (100) monolayer. The core-level spectra are shown after peak-area normalization. The origins of the recorded Al($2p$) and Ga($3d$) signals within the sample are schematically depicted as shaded regions in the inset.

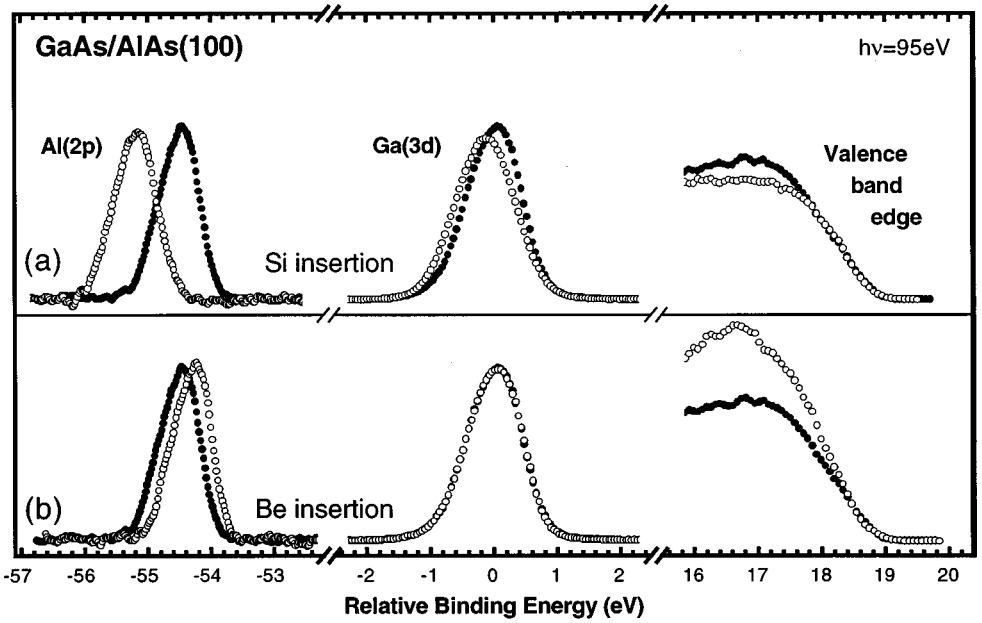

FIG. 2. Al($2p$), Ga($3d$) and valence-band-edge EDC spectra from GaAs-on-AlAs(100) heterojunctions without (solid circles) and with (open circles) an intralayer, obtained using 95-eV photons. The effects of (a) Si- and (b) Be- insertions are compared. The nominal concentration of the intralayer is 2.2×10^{14} atoms cm^{-2}. Every set of spectra from every sample has been rigidly shifted in energy to align the extreme edges of the respective valence-band spectra. The core-level spectra are shown after peak-area normalization.

signal is more bulk sensitive. As it is schematically depicted in the inset of Fig. 1, most of the Al($2p$) signal originates within a narrow portion of the AlAs buried layer, close to the GaAs/AlAs interface, while most of the Ga($3d$) signal originates within a narrow portion of the GaAs overlayer, close to the surface (shaded regions). It can be seen that upon Si insertion the Ga($3d$) peak remains at nearly the same energy position, while the Al($2p$) peak is strongly shifted toward lower kinetic energies, hence the Al($2p$)-to-Ga($3d$) energy separation increases. The core-level offset (ΔE_{CL}) measured on heterostructures without intralayer is 54.50 eV, and on Si-containing samples it amounts to 55.12 eV. These offsets refer to the energy separation measured between the centroids of the two peaks, the ''centroid'' being defined as the energy value that divides the peak into two parts of equal area. The *apparent* valence-band offset (ΔE_V^*) can be derived from the measured ΔE_{CL} offset using the equation,

$$\Delta E_V^* = \Delta E_{\mathrm{CL}} - \xi, \tag{1}$$

where

$$\xi = E_{\mathrm{Al}(2p)}^{\mathrm{AlAs}} - E_{\mathrm{Ga}(3d)}^{\mathrm{GaAs}}. \tag{2}$$

ξ amounts to 54.00 eV. This value is obtained from the binding energies known for the Al($2p$) core level in bulk AlAs [$E_{\mathrm{Al}(2p)}^{\mathrm{AlAs}} = 72.86$ eV], and for the Ga($3d$) core level in bulk GaAs [$E_{\mathrm{Ga}(3d)}^{\mathrm{GaAs}} = 18.86$ eV].[12] Hence, ΔE_V^* amounts to 0.50 eV in heterointerfaces without intralayer, and to 1.12 eV in Si-containing samples; that is, the apparent valence-band offset increases upon Si insertion, in qualitative agreement with previous x-ray photoelectron spectroscopy (XPS) reports.[12] However, the increment of ΔE_V^* observed for our GaAs/Si/AlAs(100) heterostructures (0.62 eV) is markedly larger than the value previously reported for the same—1/3 ML— intralayer concentration (0.25 eV); it is even larger than the *saturation* value previously reported for a 1/2-ML intralayer concentration (0.33 eV).[12]

Si and Be insertions were compared in another experiment, using different samples, and a different experimental station of BESSY I. Figure 2 displays Al($2p$), Ga($3d$), and valence-band-edge spectra recorded with 95-eV photons on different GaAs-on-AlAs(100) heterostructures: (i) without intralayer (solid symbols), (ii) with a Si intralayer [open symbols in Fig. 2(a)], and (iii) with a Be intralayer [open symbols in Fig. 2(b)]. The Si and Be intralayers have the same nominal concentration (2.2×10^{14} atoms cm^{-2}). Core-level intensities have been area normalized. The original *kinetic*-energy scale has been converted into a relative *binding*-energy scale, whose reference zero was arbitrarily chosen at the centroid position of the Ga($3d$) peak recorded on GaAs/AlAs(100) samples without intralayer. The variations of the Fermi-level surface pinning-position induced by the Si and Be insertions are examined in detail below. As will be later justified, the core-level energy shifts caused by such variations can be subtracted by rigidly shifting each set of spectra from the intralayer-containing samples until the leading edge of the respective valence-band spectrum coincides with the edge of the GaAs/AlAs(100) sample without intralayer. This alignment procedure was performed in Fig. 2 because it allows us to show more clearly the net variations of ΔE_{CL} caused by the intralayer insertions. The Al($2p$)-to-Ga($3d$) energy separation is observed to *increase* upon Si insertion, and to *decrease* upon Be insertion. The core-level offset measured on heterostructures without intralayer is 54.50 eV, and on Si-containing (Be-containing) samples it is 55.09 eV (54.31 eV). Hence, the *apparent* valence-band offset increases by 0.59 eV upon Si insertion, while it decreases by 0.19 eV for Be insertion. Note that the spectra displayed in Fig. 2(a) reproduce the numerical results from Fig. 1 for the effect of Si insertion in a completely independent experiment, although with a somewhat lower energy resolution.

At this stage we should justify our choice of energy alignment performed in Fig. 2 to eliminate the energy shifts caused by intralayer-induced variations of the Fermi-level surface pinning position. This is equivalent to assuming that the extreme edges of the three valence-band spectra displayed in Fig. 2 correspond to emissions originating from the

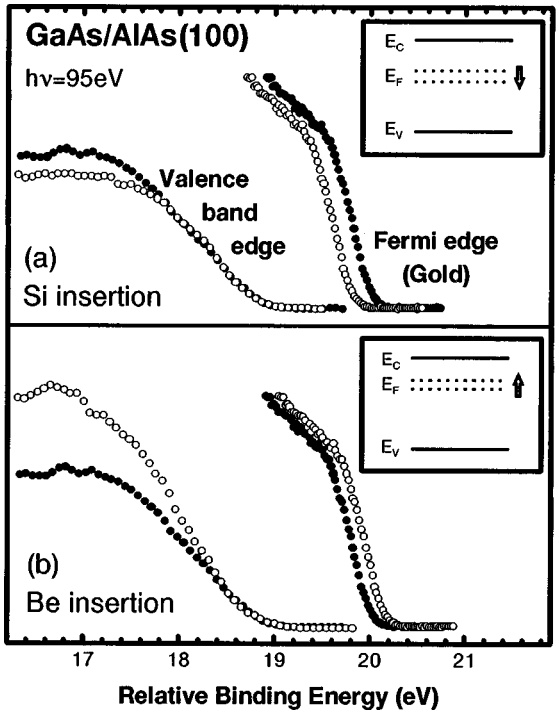

FIG. 3. Valence-band-edge spectra from GaAs-on-AlAs(100) heterojunctions without (solid circles) and with (open circles) an intralayer, and Fermi-edge spectrum from a gold foil that was in electrical contact with these samples. The effects of (a) Si and (b) Be insertions are compared. The nominal concentration of the intralayer is 2.2×10^{14} atoms cm^{-2}. The spectra were obtained using 95-eV photons, and they have been energy aligned as in Fig. 2. The shifts of the Fermi-edge spectrum displayed in the figure reflect the variations of the Fermi-level surface pinning-position occurred upon intralayer insertion, which are schematically represented in the insets.

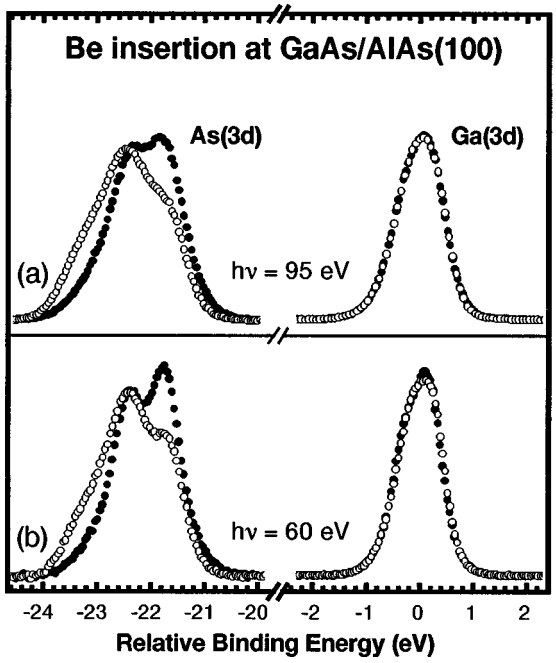

FIG. 4. As($3d$) and Ga($3d$) EDC spectra from GaAs-on-AlAs(100) heterojunctions without (solid circles) and with (open circles) a Be intralayer. The nominal concentration of the intralayer is 2.2×10^{14} atoms cm^{-2}. The spectra were obtained by illuminating the samples with (a) 95-, and (b) 60-eV photons. They have been energy aligned as in Fig. 2.

valence-band maximum (VBM) at the surface of the GaAs overlayers. Normally, at GaAs/AlAs interfaces, bands align according to the so-called type-I arrangement, with the gap of the narrow-gap material (GaAs) completely contained within the gap of the wide-gap material (AlAs). Therefore, the VBM is expected to lie at a higher position along the GaAs overlayer than along the AlAs layer. Hence, although the valence-band spectra from heterojunctions generally include overlapping features from each component, the outermost edges of the valence-band spectra displayed in Fig. 2 are expected, in this particular case, to correspond to VBM emissions from the surfaces of the respective GaAs overlayers. Such expectation is confirmed by the fact that the Ga($3d$) to valence-band-edge energy separations that can be measured in Fig. 2 correspond to the binding energy of the Ga($3d$) level (18.86 eV). Figure 3 displays the valence-band-edge spectra from the three types of GaAs-on-AlAs(100) heterostructures, along with the Fermi-edge spectrum recorded on a gold foil that was in electrical contact with the semiconductor samples. As in Fig. 2, the spectra have been rigidly shifted to align the respective valence-band extreme edges, so that the shifts of the Fermi edge displayed in the figure show the changes of the Fermi-level surface pinning position within the GaAs band gap (illustrated in the insets of Fig. 3). In GaAs/AlAs(100) heterostructures without intralayer, the surface Fermi level is observed to lie 0.95 eV above VBM; in GaAs/Si/AlAs(100) samples E_F^{surf} lies at 0.78 eV, whereas in GaAs/Be/AlAs(100) samples it lies at 1.09 eV. Hence, upon Si insertion the surface Fermi level approaches VBM by 0.17 eV, while it shifts away by 0.14 eV upon Be insertion.

As($3d$) spectra include signals coming from the GaAs and the AlAs parts of the heterostructure. Since both contributions are not easily distinguishable, As($3d$) spectra alone should not be used to determine the band alignment at GaAs/AlAs heterojunctions; such information is better extracted from the analysis of Ga($3d$) and Al($2p$) spectra. Nevertheless, the As($3d$) signal may provide additional information. The As($3d$) spectra from our Si-containing junctions are simply broader than those from the heterostructures without intralayer. However, the As($3d$) spectra from Be-containing junctions reveal a pronounced modification. This is shown in Fig. 4, which displays As($3d$) and Ga($3d$) spectra recorded on GaAs/AlAs(100) heterostructures with a Be intralayer (open symbols), and without it (solid symbols). Similar As($3d$) peak-shape changes are observed using 95- and 60-eV photons (Fig. 4), which correspond to surface- and bulk-sensitive conditions, respectively. Without performing any deconvolution analysis, it can be observed from the raw data that a distinct extra emission appears in the *high*-binding-energy side of the As($3d$) peak recorded on Be-containing heterostructures. Taking into account our Ga($3d$) and Al($2p$) data, such extra component cannot be consistently associated with either an emission from bulk GaAs, or an emission from bulk AlAs, shifted in energy relative to the corresponding emission in samples without intralayer because of an electronic mechanism (band-offset or band-bending change). If the shifted As($3d$) emission was to be

connected with an emission from bulk GaAs, then a similar shift should be observed for the bulk Ga($3d$) signal. Figure 4 shows that this does not occur. On the contrary, the Ga($3d$) core-level spectra from heterojunctions with and without a Be intralayer are nearly identical. If the extra As($3d$) emission was emanating from bulk AlAs, then a similar shift should be observed on the Al($2p$) peak. Again, our experimental results do not confirm such a behavior, since the shifts of this As($3d$) component and of the corresponding Al($2p$) peak have *opposite* signs (Figs. 2 and 4). It appears thus that the As($3d$) line-shape changes observed upon Be insertion have mainly a *chemical* origin rather than an electronic one. Moreover, the insensitivity observed in the As($3d$) emission to variations of the probing depth suggests a *bulk* origin for the extra component, rather than a surface or interface origin. Then, such component can be tentatively associated with emissions from arsenic atoms located all along the overlayer region, in a modified environment resulting from beryllium out-diffusion processes.

Recently, Wilks *et al.* have reported[22] a photoemission study on the effect of 1-ML-thick Si and Be intralayers at GaAs-on-$Al_{0.8}Ga_{0.2}As$(100) heterojunctions. They reported[22] As($3d$) line-shape changes quite similar to those we have found for our GaAs-on-AlAs(100) structures upon insertion of 1/3-ML-thick Si and Be intralayers. In contrast with our interpretation, they assign the As($3d$) line-shape changes observed for Be insertion to a modification of the valence-band offset by -0.52 eV.[22] Since their study is based on the As($3d$) line, they have to revert to a line-shape analysis in order to extract what they suggest is the contribution from either side of the heterojunction, by assuming that chemical components are small and confined to the interface region.[22] In contrast, our study does not rely on line-shape analysis and its underlying assumptions. Rather, we use the Ga($3d$) and Al($2p$) peaks, since each of these signals is restricted to one side of the interface. As mentioned above, in our case the Ga($3d$)-to-Al($2p$) offset is reduced upon Be insertion by 0.19 eV. Considering the As($3d$), Ga($3d$), and Al(2p) data displayed in Figs. 2 and 4, it is clear that the As($3d$) line-shape changes we have observed upon Be insertion cannot be interpreted in terms of electronic variations. It seems that there are chemically induced changes in the As($3d$) line shape, which are bound to seriously affect the analysis of the data by Wilks *et al.*[22] in terms of band-offset changes.

IV. DISCUSSION

The most important issue in interpreting the core-level shifts displayed in Figs. 1 and 2 is to elucidate whether they can be unambiguously related to band-offset changes, as previously reported. Although a change of the interface band offset can certainly modify the measured Al($2p$)-to-Ga($3d$) energy separation, a change of this core-level offset does not necessarily imply a band-offset modification. For instance, as will be shown in detail below, this separation can be affected by variations in the band-bending profile. Hence, the interpretation of such core-level data is not unique. The experimental results presented in the preceding section have revealed an opposite behavior of the core-level separation and surface Fermi-level position for Si and Be insertions, which is qualitatively consistent with an explanation in terms of band-bending effects and a doping role of the inserted impurities. In the following, we examine whether the ''band-bending'' interpretation is also quantitatively consistent with our experimental results.

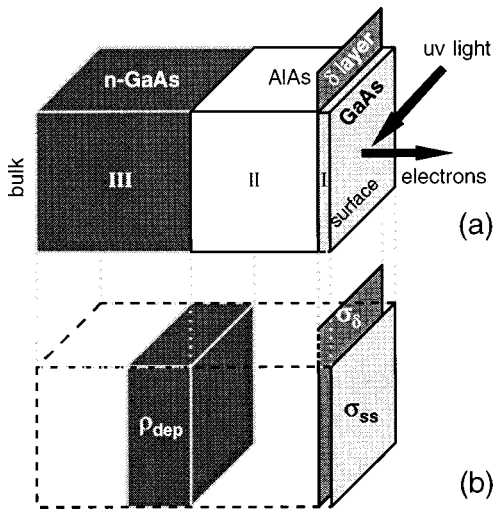

FIG. 5. (a) Schematic representation of the sample structure. (b) Model charge configuration assumed in our calculations.

As illustrated in Fig. 5(a), our samples include three well distinguished regions: (i) the GaAs *n*-doped substrate (region III), (ii) the AlAs buried layer (region II), and (iii) the GaAs overlayer (region I). Some samples contain a Si or a Be δ layer inserted at the interface position, between regions I and II. The band profile along the different regions can be calculated by solving the Poisson equation for the charge distribution that corresponds to each type of sample, including the appropriate charge neutrality and boundary conditions. The summation of the potential variations along every region must equal the magnitude of the band bending across the entire semiconductor structure, which is a known parameter given by the difference between the energy positions of the Fermi level deep in the bulk and at the surface. Due to the high *n*-type doping of the substrate ($n=10^{18}$ cm^{-3}), in all the samples the Fermi level lies close to the conduction-band minimum (CBM) deep in the bulk. However, its position at the surface has been experimentally determined to be different for each of the three types of heterostructures considered (Fig. 3).

We have calculated the band profile in heterostructures without intralayer by assuming the following charge distribution: (i) a charged-sheet located at the surface, representing the charge trapped in surface states (σ_{SS}), and (ii) a carrier-depleted charged-volume located at the shallowest part of the Si-doped GaAs substrate, which consists of a homogeneous distribution of positively ionized Si atoms (ρ_{dep}); see Fig. 5(b). The corresponding band profile is displayed in Fig. 6(a). It can be seen that band bending takes place mainly along the AlAs buried layer, and that the potential varies very little along the GaAs overlayer, by only 0.03 V. Thus, this calculation confirms that in heterostructures without an intralayer the overlayer bands are nearly flat, as usually assumed in PES determinations of band offsets.[23]

When accounting for the doping character of Si and Be in GaAs, it seems plausible that the above band profile may be modified by the insertion of intralayers. We have assumed

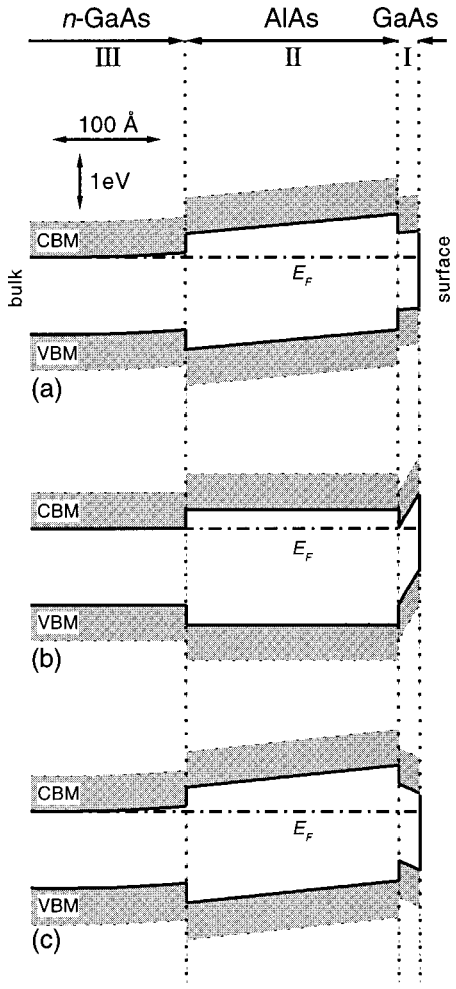

FIG. 6. Band profiles of our (a) GaAs/AlAs(100), (b) GaAs/Si/AlAs(100), and (c) GaAs/Be/AlAs(100) heterostructures. They have been calculated considering the model and assumptions described in the text. An efficient doping concentration of 2.39×10^{13} cm^{-2} has been assumed for the case of Si, and of 7.4×10^{12} cm^{-2} for the case of Be.

that in our intralayer-containing samples a part of the inserted atoms plays a *doping* role; that is, a certain fraction of the inserted Si (Be) atoms is positively (negatively) ionized, electrons (holes) having been released to the host semiconductor lattice. Such a fraction will be called ''efficient doping concentration.'' Although the exact final distribution of the intralayer atoms is unknown, and some segregation and out-diffusion is expected to occur, a certain fraction of the inserted atoms is likely to remain localized at the interface position. For simplification, we have assumed that all intralayer atoms acting as dopants (efficient doping concentration) are confined at the interface position. This assumption is quite strong, and is not expected to exactly match the real situation, since some of the out-diffused atoms could also have a doping role. Therefore, the results discussed below, of simple calculations that we have performed based upon the above assumptions, should be regarded only as illustrative ones. Any experimental result that could provide additional information on the real atomic distribution in this type of samples would be of great importance to achieve more accurate calculations.

Theoretical calculations have shown that the incorporation of a Si-δ-layer in bulk GaAs induces a V-shaped potential, which confines the impurity electrons within the plane of the dopants. Such calculations are performed by self-consistently solving the Schrödinger and Poisson equations; the impurity electrons are usually represented by plane-wave functions, and the δ layer is seen as inserted within an infinite solid. The proximity of a surface considerably alters the properties of δ-doped layers.[24] As the δ layer gets close to a surface, an increasing fraction of impurity electrons becomes trapped in surface states. Sampaio *et al.* calculated[24] that about 45% of the impurity electrons are at the surface for a Si-δ-layer located 200 nm away from the surface and with a concentration of 7×10^{11} cm^{-2}. Experimental results have also shown that the position of the δ layer with respect to the surface is an important parameter. For instance, the intensity of reflectance-anisotropy-spectroscopy (RAS) features has been found to vary with the position of the δ plane from the GaAs surface.[25] In our samples, the δ layer has been inserted at the GaAs/AlAs interface, which is located 2 nm away from the surface. According to the hydrogen model, the first-orbit radius of impurity electrons in GaAs amounts to 10 nm. Thus, in our case, due to the close proximity of the surface, it is unlikely that the impurity electrons provided by the Si intralayer may move freely along the interface. On the contrary, most of them are probably trapped in surface states. The same types of arguments can be applied to the case of Be, but considering holes instead of electrons. We are then essentially faced with an electrostatic problem, and in order to calculate the band profiles in our intralayer-containing heterostructures we have thus considered a static, *capacitorlike*, charge distribution [schematically depicted in Fig. 5(b)], where the electrons (holes) provided by the intralayer are *separated* from their parent Si (Be) atoms, and trapped in surface states. This sample charge distribution is similar to the one considered for heterostructures without intralayer, but includes also a positively (negatively) charged sheet (σ_δ), located at the interface position, which represents the charge from ionized Si (Be) atoms. Note that the charges at the surface and at the carrier-depleted region of the substrate are modified to satisfy the charge-neutrality condition.

The band profile in intralayer-containing samples depends on the amount of *ionized* intralayer atoms. The band bending across the overlayer region can be calculated for a fixed intralayer charge density, or conversely, one can calculate the intralayer charge density that produces a certain potential variation across the overlayer. We have calculated the amount of ionized intralayer atoms required to induce a variation in the magnitude of the overlayer band bending that equals the changes observed in the Al($2p$)-to-Ga($3d$) offset displayed in Fig. 2. According to our calculations, a concentration of 2.39×10^{13} atoms cm^{-2} (7.4×10^{12} atoms cm^{-2}) must be positively (negatively) ionized to account for the experimental results obtained for insertion of Si (Be). Figures 6(b) and 6(c) display the band profiles calculated for heterostructures containing intralayer charged sheets with the above concentrations. It can be seen that the *n*-type Si δ layer induces a sharp *upward* overlayer band bending, while the *p*-type Be δ layer causes a *downward* overlayer band bending. Hence, according to the above model, the band profiles in GaAs/AlAs heterojunctions located close to a surface, and containing a Si or a Be intralayer, do not correspond to

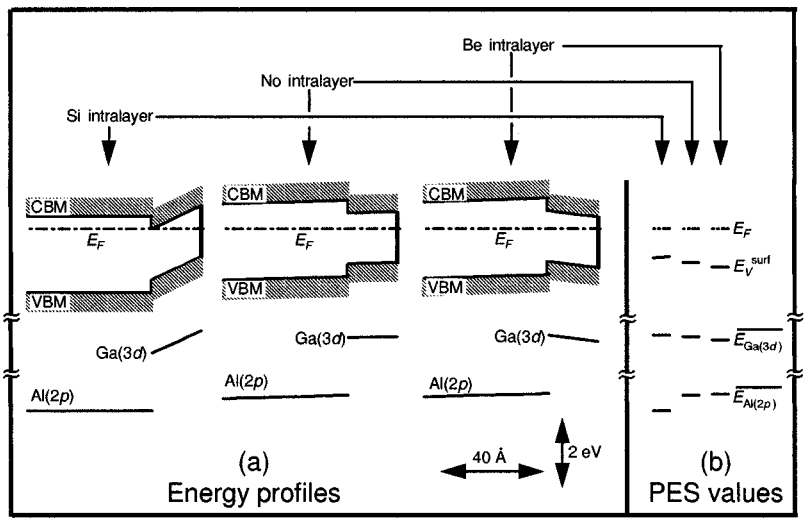

FIG. 7. (a) Close up view of the band diagrams displayed in Fig. 6, focusing on the region close to the surface, and depth profiles of the corresponding Al($2p$) and Ga($3d$) levels. (b) Average energy values expected to be obtained from PES measurements, performed under the experimental conditions of Fig. 2, on heterostructures with the energy profiles of Fig. 7(a).

the ''normal'' situation of flat overlayer bands, which occurs in heterostructures without intralayer. On the contrary, the intralayer insertion induces a significant bending of the overlayer bands.

In order to understand how such intralayer-induced modifications of the band profile can alter the Al($2p$)-to-Ga($3d$) energy separation measured by PES, we need to take into account that photoemission does not only probe the interface region, but adds up signals coming from atoms located at different depths. Each contribution is weighted by an exponential factor, which accounts for the attenuation of the signal due to the electron scattering, so that the PES average energy of a core level $\overline{E_{CL}}$ can be written as follows:

$$\overline{E_{CL}} = \frac{\int_0^\infty E_{CL}(z)\exp(-z/\lambda)dz}{\int_0^\infty \exp(-z/\lambda)dz}, \qquad (3)$$

where $E_{CL}(z)$ describes the energy value of the core level as a function of the depth z, and λ is the photoelectron attenuation length. Hence, PES probes a certain volume of the sample close to the surface, enhancing the signals coming from shallow regions over those originating in the deep layers. Figure 7(a) shows a close-up view of the band profiles displayed in Fig. 6, focusing on the region of interest for photoemission, that is, the entire GaAs overlayer, and the shallowest portion of the AlAs buried layer. The figure includes the $E_{CL}(z)$ profiles of the Al($2p$) and Ga($3d$) core levels, which suffer energy variations with depth parallel to those of the VBM and CBM levels. Since the Al($2p$) and Ga($3d$) energy profiles are different for each type of heterostructure, the respective PES average values will vary, which may result in a change of the Al($2p$)-to-Ga($3d$) offset. This situation is shown in Fig. 7(b), where we have represented the energy values expected to be obtained from PES measurements, performed using 95-eV photons, on GaAs/AlAs, GaAs/Si/AlAs, and GaAs/Be/AlAs heterostructures with the energy profiles displayed in Fig. 7(a). The E_V^{surf} value represented in Fig. 7(b) corresponds to the position of the VBM at the surface. The shifts of E_V^{surf} relative to E_F reflect the changes of the Fermi-level surface pinning-position upon Si and Be insertions as determined experimentally (Fig. 3); the E_V^{surf} values have been introduced as inputs in the band-profile calculations. The PES average values of the Al($2p$) and Ga($3d$) core levels displayed in Fig. 7(b) have been calculated according to Eq. (3), by using the attenuation lengths that correspond to the experimental conditions of Figs. 1 and 2 (95-eV photons). It can be seen that the PES average energy of the Ga($3d$) core level $\overline{E_{Ga}(3d)}$ essentially corresponds to its value at the surface, being scarcely sensitive to any energy variation existing along the GaAs overlayer. Analogously, the PES average energy of the Al($2p$) core level $\overline{E_{Al}(2p)}$ corresponds to its value at the shallowest part of the AlAs region, being scarcely sensitive to the energy variations along the AlAs buried layer. Remarkably, $\overline{E_{Al(2p)}}$ is much more sensitive to changes of the overlayer band bending than $\overline{E_{Ga(3d)}}$; in fact, $\overline{E_{Al(2p)}}$ is shifted by the same energy amount as the magnitude of the entire overlayer band-bending change. The small differences between the $\overline{E_{Ga(3d)}}$ energies for the three heterostructures considered here are mainly a consequence of variations in the Fermi-level surface pinning position; note that the shifts of $\overline{E_{Ga(3d)}}$ follow the trend of E_V^{surf}. Figure 7 shows that the upward (downward) bending of all the overlayer energy levels, induced by Si (Be) insertion, results in a larger (shorter) value of the Al($2p$)-to-Ga($3d$) energy distance measured by PES.

The above model enables us to explain the observed core-level offset variations (Figs. 1 and 2) solely on the basis of intralayer-induced modifications of the overlayer band bending, with no need to include any change of the interface band offset. Moreover, this model not only reproduces the sign and magnitude of the changes observed in the energy separation measured between the Al($2p$) and Ga($3d$) peaks, but also the individual behavior of each core level. This can be verified by looking at Fig. 1, where the spectra corresponding to samples with and without a Si intralayer are displayed so as the respective Fermi energies coincide, as occurs in Fig. 7(b). It can be seen that, upon Si insertion, the Ga($3d$) peak does not move significantly, just slightly toward higher kinetic energies, while the Al($2p$) peak is widely shifted

toward lower kinetic energies. This is just the behavior predicted by our PES calculations [see Fig. 7(b)]; however, it contrasts with certain arguments invoked[1] to invalidate the ''band-bending'' interpretation.[14,15] Franciosi and Van de Walle stated[1] that in AlAs-on-GaAs heterojunctions ''changes in band bending should affect only the apparent Al($2p$) binding energy and line shape, and not the Ga($3d$) position,'' which is equivalent to say that variations of the overlayer band bending should affect the core-level peak from the overlayer, and not the peak from the buried layer. Such a statement is contrary to the results of our PES average-energy calculations discussed above for the reverse GaAs-on-AlAs stacking sequence, and seems to be incorrect. In fact, the experimental behavior we have observed for the energy positions of the individual core levels, relative to the Fermi level, strongly supports the band-bending interpretation.

It has been argued[1] that ''as far as the Fermi-level position is concerned, variations in band bending from sample to sample result in a *rigid* shift of the core levels.'' However, as we have shown above, changes of the pinning position of the Fermi level at the surface, and of the magnitude of the band bending across the overlayer, may both occur upon intralayer insertion, but produce different effects. The Fermi-level surface pinning-position determines the magnitude of the band bending across the *entire* semiconductor structure and, if bands remain flat within the PES probing depth, its variation produces only a rigid shift of the whole set of EDC spectra relative to E_F. However, a change of the magnitude of the band bending across the *overlayer* may alter the energy separation measured between core levels from both sides of the interface (see Fig. 7). The variations of the Fermi-level surface pinning-position experimentally observed here (Fig. 3) are not random, but follow the trend that can be expected from the theoretical work of Sampaio *et al.*[24] Their calculations on the properties of Si δ-doped layers at different distances from the surface, indicate that (i) the amount of impurity electrons trapped in surface states increases as the δ layer gets closer to the surface, and that (ii) the surface Fermi level approaches the VBM when the electronic charge trapped in surface states increases.[24] Therefore, the electronic charge trapped in surface states can be expected to be higher (lower) in heterostructures containing an *n*-type (*p*-type) intralayer close to the surface, than in heterostructures without such intralayer, and consequently the surface Fermi level can be expected to approach (to move away from) the VBM upon insertion of a *n*-type (*p*-type) intralayer. This is indeed what has been observed experimentally (Fig. 3).

Franciosi and Van de Walle have argued[1] that ''for the band-bending picture to work, all of the Si atoms deposited at the interface should out-diffuse in the overlayer and act as donors (unity activation).'' They explained[1] the band-bending effect in AlAs-on-GaAs heterojunctions as follows: ''preferential Si out-diffusion toward the surface produces a highly degenerate *n*-type III-V overlayer with an anomalously short Debye length; this, together with Fermi-level pinning near midgap at the surface, would preferentially localize band bending in the overlayer.'' They cite[1] that ''the Debye length required to sustain such a band bending within relatively thin overlayers would require a doping of the order of $(1-5)\times10^{20}$ cm^{-3} within the III-V overlayer, which exceeds by several orders of magnitude the highest doping levels ever achieved in AlAs.'' In that respect we would like to notice that the cause of the band bending *is not* the segregation and/or outdiffussion of Si intralayer atoms. Within our interpretation the overlayer band bending results from the trapping of carriers in surface states, which separates the carriers provided by the intralayer from their ionized parent atoms. *Bulk* doping is not necessary for band bending to exist, just a separation of charges needs to take place. Therefore, when discussing the band-bending interpretation, it is more appropriate to speak of *sheet* rather than *bulk* doping concentration. Segregation of intralayer atoms, rather than being the cause, *is a consequence* of the overlayer band bending. Segregation is thought to occur in part because the ionized intralayer atoms try to move during growth toward the surface driven by the high electric field associated to the surface band bending.[26]

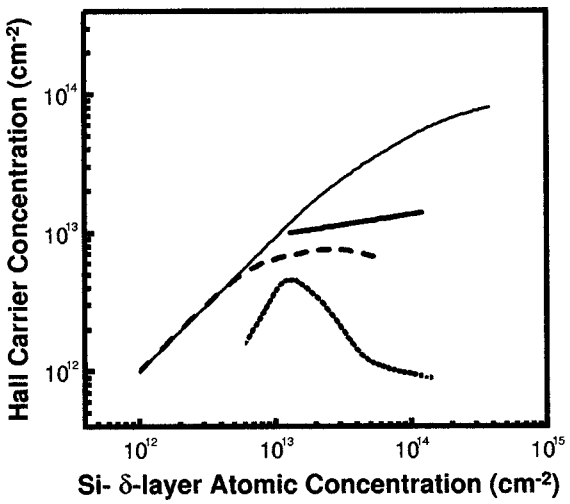

FIG. 8. Hall-effect results reported for Si δ layers in GaAs(100). The sheet carrier concentration is represented as a function of the nominal δ-layer atomic concentration for different Si-insertion methods: (i) continuous Si deposition at substrate temperature $T=400$ °C and GaAs overgrowth at $T=400$ °C (dotted line) (Ref. 27), (ii) continuous Si-deposition at $T=590$ °C and GaAs overgrowth at $T=590$ °C (dashed line) (Ref. 28), (iii) pulsed low-flux Si deposition at $T=590$ °C and GaAs overgrowth at at $T=540$ °C (thick-solid line) (Ref. 20), and (iv) pulsed low-flux Si deposition at $T=590$ °C and GaAs overgrowth at $T=590$ °C (thin-solid line) (Ref. 21).

From the above model calculations we infer that about 2×10^{13} atoms cm^{-2} (7×10^{12} atoms cm^{-2}) must be ionized in the intralayer to account for the Al($2p$)-to-Ga($3d$) offset variations observed upon Si (Be) insertion on the basis of a band-bending effect. Such *efficient doping* concentration has a direct relation to the *free-carrier* concentration determined by Hall-effect measurements. Figure 8 summarizes Hall-effect results reported for Si δ layers in GaAs(100).[27,28,20,21] It can be seen that, for diverse growth recipes, the carrier concentration increases with the δ-layer atomic concentration up to a nominal atomic concentration of about $(1-3)\times10^{13}$ atoms cm^{-2}. For higher δ-layer atomic concentrations, the carrier concentration attained depends critically on growth conditions. If the δ layer is in-

serted by using a *continuous* deposition method, the carrier concentration decreases, more or less abruptly, after reaching a saturation value (Fig. 8). However, in the present work, a *pulsed low-flux* impurity-deposition recipe has been used. This method minimizes Si clustering, thus avoiding the abrupt diminution of the carrier-concentration efficiency.[20,21] Figure 8 shows that carrier concentrations in the 10^{13}-cm^{-2} range are readily achieved for Si δ layer atomic concentrations in the (high-10^{13}/low-10^{14})-atoms cm^{-2} range if a ''pulsed low-flux'' impurity deposition recipe is used. Thus, the efficient doping concentrations necessary to explain the experimental results on the basis of a band-bending effect can be readily achieved, contrary to what has been argued.[1]

We have shown above how the changes induced in the line energies of Al($2p$) and Ga($3d$) PES spectra from GaAs/AlAs(100) junctions by insertion of Si or Be can be successfully explained in terms of band-bending effects. The observed changes would be essentially produced by the combination of two mechanisms: (i) the doping behavior of a part of the inserted atoms, and (ii) the trapping of the generated carriers at surface states. The ''overlayer capacitor'' model we have used to illustrate the band bending interpretation differs substantially from the ''interface capacitor'' model previously invoked to explain intralayer-induced band-offset changes. The band-bending interpretation provides a straightforward explanation for the fact that Si and Be intralayers induce changes of opposite sign: this can be easily understood accounting for the respective *n*-type and *p*-type doping behavior. However, such an experimental observation cannot be so readily explained within the framework of the interface-capacitor model. In fact, such a model does not provide an easy interpretation for the changes observed upon Be insertion in terms of band-offset variations. The reason is that Be has not an amphoteric behavior, and consequently, the establishment of interface dipoles in this case does not have such a straightforward explanation as for the case of Si.

The polarity nature of the interface plays a key role within the interface-capacitor model, but it is not important for the model here proposed as long as the properties of the growth on different substrate orientations do not change the efficient doping concentration. Core-level offset changes have been observed upon Si insertion in polar and nonpolar interfaces.[15,17] Whereas this observation can be well understood within the band-bending interpretation, the interface capacitor model cannot explain it, because, according to this model, band-offset changes are not expected to occur for nonpolar orientations.[10,16,17] Previously, we have observed Si-induced core-level offset variations that are larger for polar GaAs/AlAs(100) junctions than for nonpolar GaAs/AlAs(110) ones.[17] This result can be well understood within the band-bending interpretation, since the strength of the overlayer-capacitor effect depends on the *efficient doping* concentration of the intralayer; this one is expected to be higher in (100)-oriented samples than in (110)-oriented ones, for two reasons: (i) because self-compensation is known to be more important for growth on (110) substrates,[29] and (ii) because the Si-insertion recipe used here was specifically optimized for growth on (100) surfaces.[20] The core-level offset variation that we have observed upon Si insertion at GaAs-on-AlAs(100) junctions is remarkably larger than the changes previously reported by other groups.[30] Such an observation can be also explained within the band-bending interpretation: the larger effect is likely due to the higher doping efficiency of our pulsed low-flux Si-deposition technique, in comparison with the growth recipes employed by other groups (see Fig. 8). It should also be noted that although the position of the intralayer with respect to the surface is irrelevant within the interface-capacitor model, it plays a key role within our overlayer-capacitor model. No differences in the strength of the microscopic interface capacitor are in principle expected between the samples used in PES experiments and in devices. However, charge separation in the overlayer and the associated band bending occurs only if a certain amount of the carriers generated by the intralayer insertion becomes trapped in surface states, which requires that the intralayer is located close enough to the surface. Although such a condition is easily fulfilled in the samples typically analyzed in a photoemission experiment, it is not so clear the relevance of this effect for the type of heterojunctions with deeply buried interfaces that are generally used in devices.

V. CONCLUSIONS

Insertion of Si and Be intralayers at GaAs-on-AlAs(100) interfaces has been investigated by photoelectron spectroscopy (PES) using synchrotron radiation. The results obtained are consistent with the doping behavior typically exhibited by the inserted impurities, and can be well understood considering the *overlayer capacitor* effect caused by (i) the ionization of a part of the intralayer atoms, and (ii) the trapping of the generated carriers at surface states. The core-level offset changes observed upon Si and Be insertions can be fully explained without including any change of the interface band offset, simply by considering the changes of the *band-bending profile* that take place in connection with the variations of the overlayer capacitance.

ACKNOWLEDGMENTS

We gratefully acknowledge P. Schützendübe and H. P. Schönherr for their expert MBE assistance, W. Braun for the flexibility in the beam-time scheduling, necessary to coordinate the synchrotron experiments performed in BESSY with the MBE sample growth, I. Jiménez, N. Franco, C. Polop, S.-A. Ding, and S. Barman for technical assistance during the synchrotron beam-times, and H. Kostial, H. Yang, and A. Yamada for valuable discussions. One of us (M.M.) acknowledges the financial aid from the *Comunidad Autónoma de Madrid* (Spain) and the hospitality extended to her during her visit to the *Paul-Drude-Institut*. This work was partially supported by the Spanish *Dirección General de Investigación Científica y Técnica* under Grant Nos. PB94-53 and PB94-1530. The work at BESSY was supported by the EU Human Capital and Mobility Programme under Contract No. CHGE-CT93-0027. The work at LURE was supported by the EU Large Scale Installations Programme, Project No. SP-207.

*Electronic address: mmoreno@icmm.csic.es

[1] A. Franciosi and C. G. Van de Walle, Surf. Sci. Rep. **25**, 1 (1996).
[2] K. Ploog, A. Fischer, and E. F. Schubert, Surf. Sci. **174**, 120 (1986).
[3] K. Ploog, J. Cryst. Growth **81**, 304 (1987).
[4] E. F. Schubert, J. Vac. Sci. Technol. A **8**, 2980 (1990).
[5] F. Capasso, K. Mohammed, and A. Y. Cho, J. Vac. Sci. Technol. B **3**, 1245 (1985).
[6] G. Muller, A. Zrenner, F. Koch, and K. Ploog, Appl. Phys. Lett. **55**, 1564 (1989).
[7] E. F. Schubert, L. W. Tu, G. J. Zydzik, R. F. Kopf, A. Benvenuti, and M. R. Pinto, Appl. Phys. Lett. **60**, 466 (1992).
[8] A. Muñoz, N. Chetty, and R. M. Martin, Phys. Rev. B **41**, 2976 (1990).
[9] M. Peressi, S. Baroni, R. Resta, and A. Baldereschi, Phys. Rev. B **43**, 7347 (1991).
[10] W. A. Harrison, E. A. Kraut, J. R. Waldrop, and R. W. Grant, Phys. Rev. B **18**, 4402 (1978).
[11] R. W. Grant, E. A. Kraut, S. P. Kowalczyk, and J. R. Waldrop, J. Vac. Sci. Technol. B **1**, 320 (1983).
[12] L. Sorba, G. Bratina, G. Ceccone, A. Antonini, J. F. Walker, M. Micovic, and A. Franciosi, Phys. Rev. B **43**, 2450 (1991).
[13] M. Marsi, R. Houdre, A. Rudra, M. Ilegems, F. Gozzo, C. Coluzza, and G. Margaritondo, Phys. Rev. B **47**, 6455 (1993).
[14] M. Akazawa, H. Hasegawa, H. Tomozawa, and H. Fujikura, Jpn. J. Appl. Phys., Part 2 **31**, L1012 (1992).
[15] Y. Hashimoto, G. Tanaka, and T. Ikoma, J. Vac. Sci. Technol. B **12**, 125 (1994).
[16] S. Baroni, R. Resta, and A. Baldereschi, in *Proceedings of the 19th International Conference on the Physics of Semiconductors*, edited by W. Zawadzki (Institute of Physics, Polish Academy of Sciences, Wroclaw, 1988), p. 525.
[17] M. Moreno, H. Yang, M. Höricke, M. Alonso, J. A. Martín-Gago, R. Hey, K. Horn, J. L. Sacedón, and K. H. Ploog, Phys. Rev. B **57**, 12 314 (1998).
[18] T. Ogama, J. Appl. Phys. **64**, 753 (1988).
[19] G. Margaritondo, F. Gozzo, and C. Coluzza, Phys. Rev. B **47**, 9907 (1993).
[20] L. Däweritz, H. Kostial, R. Hey, M. Ramsteiner, J. Wagner, M. Maier, J. Behrend, and M. Höricke, J. Cryst. Growth **150**, 214 (1995).
[21] K. H. Ploog and L. Däweritz, Jpn. J. Appl. Phys., Part 1 **34**, 691 (1995).
[22] S. P. Wilks, S. Burgess, P. Dunstan, M. Pan, M. A. Pritchard, R. H. Williams, D. Cammack, S. A. Clark, and D. I. Westwood, Appl. Surf. Sci. **123/124**, 528 (1998).
[23] E. A. Kraut, R. W. Grant, J. R. Waldrop, and S. P. Kowalczyk, Phys. Rev. B **28**, 1965 (1983).
[24] J. F. Sampaio, S. L. S. Freire, and E. S. Alves, J. Appl. Phys. **81**, 530 (1997).
[25] Z. Sobiesierski, D. I. Westwood, and M. Elliott, Phys. Rev. B **56**, 15 277 (1997).
[26] E. F. Schubert, J. M. Kuo, R. F. Kopf, A. S. Jordan, H. S. Luftman, and L. C. Hopkins, Phys. Rev. B **42**, 1364 (1990).
[27] M. J. Ashwin, M. Fahy, J. J. Harris, R. C. Newman, D. A. Sansom, R. Addinall, D. S. McPhail, and V. K. M. Sharma, J. Appl. Phys. **73**, 633 (1993).
[28] K. Kohler, P. Ganser, and M. Maier, J. Cryst. Growth **127**, 720 (1993).
[29] J. M. Ballingall and C. E. C. Wood, J. Vac. Sci. Technol. B **1**, 162 (1983).
[30] See Fig. 3 of Ref. 17.